PPPL-2363

UC20-A,D,F

I-27888

PPPL-2363

D, 1933-X

177 9/12/86 W.B.

(2) (25)

POWER TRANSPORT TO THE PDX SCOOP LIMITER

PPPL--2363

DE86 015513

By

H.W. Kugel et al.

JULY 1986

PLASMA PHYSICS LABORATORY

PRINCETON UNIVERSITY

PRINCETON, NEW JERSEY

PREPARED FOR THE U.S. DEPARTMENT OF ENERGY, UNDER CONTRACT DE-AC02-76-CHO-3073.

NOTICE

Printed in the United States of America

Available from:

National Technical Information Service
U.S. Department of Commerce
5285 Port Royal Road
Springfield, Virginia 22161

Price Printed Copy $ __*__ ; Microfiche $4.50

*Pages	NTIS Selling Price
1-25	$7.00
25-50	$8.50
51-75	$10.00
76-100	$11.50
101-125	$13.00
126-150	$14.50
151-175	$16.00
176-200	$17.50
201-225	$19.00
226-250	$20.50
251-275	$22.00
276-300	$23.50
301-325	$25.00
326-350	$26.50
351-375	$28.00
376-400	$29.50
401-425	$31.00
426-450	$32.50
451-475	$34.00
476-500	$35.50
500-525	$37.00
526-550	$38.50
551-575	$40.00
567-600	$41.50

For documents over 600 pages, add $1.50 for each additional 25-page increment.

POWER TRANSPORT TO THE PDX SCOOP LIMITER

H. W. Kugel, K. Bol, R. Budny, R. Fonck, R. Goldston, B. Grek, R. Kaita,
S. Kaye, R. J. Knize, D. Manos, R. McCann, D. McCune, K. McGuire,
M. Okabayashi, D. K. Owens, D. Post, G. Schmidt, and M. Ulrickson
Plasma Physics Laboratory, Princeton University
Princeton, New Jersey 08544

ABSTRACT

Power transport to the PDX graphite scoop limiter was measured during both ohmic- and neutral-beam-heated discharges by observing its front face temperatures using an infrared camera. Measurements were made as a function of plasma density, current, position, fueling mode, and heating power for both co- and counter-neutral beam injection. The measured thermal load on the scoop limiter was 25-50% of the total plasma heating power. The measured peak front face midplane temperature was 1500 ^{0}C corresponding to a peak surface power density of 3 kW/cm^2. This power density implies an effective parallel power flow of 54 kW/cm^2 in agreement with the radial power distribution extrapolated from TVTS and calorimetry measurements. Symmetric and asymmetric thermal loads were observed. The asymmetric heat loads were predominantly skewed toward the respective ion drift directions for both co- and counter-injected beams. The results of transport calculations are consistent with the direction and magnitude of the observed asymmetries.

1.0 INTRODUCTION.

Mechanical pump limiters are currently under extensive investigation as simpler alternatives to magnetic divertors for recycling control, impurity reduction, increased edge power control, and achieving high confinement times in fusion plasmas.[1-3] A special embodiment of mechanical limiter concepts, called a particle scoop limiter, was studied in the PDX tokamak during a brief series of experimental runs. The scoop limiter was clad with a graphite front face and backed by a 50 liter volume for collecting particles. Figure 1 gives a schematic diagram of the scoop limiter showing the pump channels, neutralizer, and diagnostics. Figure 2 gives a schematic view of the scoop limiter front face. Measurements were made with both ohmic- and beam-heated plasmas. Up to 5 MW of D^0 power were used to heat PDX D^+ plasmas at line average densities up to 8×10^{13} cm^{-3} and plasma currents up to 450 kA. Neutral densities inside the plenum were of order 5×10^{14} cm^{-3}. Plasma densities of typically 2×10^{12} cm^{-3} were measured in the scoop limiter channels. The scoop limiter neutral-beam-heated discharges exhibited higher energy and particle confinement times than observed in similar plasmas with standard rail limiter discharges. Detailed discussions of the general experimental results and analysis are given elsewhere.[4-8] In this paper, we present results on power transport to the PDX scoop limiter, as derived from infrared camera measurements of its front face midplane temperatures, during ohmic- and neutral-beam-heated discharges.

2.0 EXPERIMENTAL PROCEDURE.

A scanning infrared camera (Inframetrics 210) was used to view the front graphite face of the PDX scoop limiter from a distance of about 3.2 m through a ZnSe window. The infrared camera was operated in the 3-5 µm wavelength range, and could be used in a standard video mode or in a line-scan mode in which the temperature was recorded along a horizontal line at the midplane of the limiter front surface. The time response of the system was 125 µs and a scan was taken every 3 ms. A scan was computer archived every 3 ms or video recorded every 30 ms. The system detection efficiency was calibrated off-line using a standard commercially available IR Black Body source. The emissivity of the limiter graphite surface was determined by circulating hot water (50 ^{0}C) through the limiter cooling lines and comparing the detected infrared signal to the limiter thermocouples. In addition, a sample of the same type of graphite (ATJ) was heated in a furnace to 150 ^{0}C, and the emitted infrared signal was detected through the experimental geometry and compared to contact thermocouple temperature measurements. The results were independent of position and consistent with an average emissivity of 0.98. The incident surface power densities were derived from the temperatures measured in the line-scan mode using standard theoretical heat conduction calculations with temperature-dependent material parameters. The camera video mode was used for surveys of the entire limiter front surface and to verify that the surface temperatures observed in the line-scan mode load were symmetric about the midplane.

3.0 RESULTS.

3.1 Thermal Loads and Power Transport.

Typical ohmic-heated plasmas with plasma currents of 350 kA and densities of 5×10^{13} cm^{-3} produced peak midplane scoop limiter front face temperatures of 245 ^{0}C corresponding to peak power densities of 0.35 kW/ cm^2. During neutral-beam-heated discharges with comparable plasma currents and densities and injected powers up to 5.2 MW, the observed peak midplane front face temperatures were 1500 ^{0}C, corresponding to incident power densities of 3 kW/cm^2. Typically, the scoop limiter front face thermal load varied from 25 to 50 % of the total heating power (OH + NBI) absorbed by the plasma depending on the operating conditions.

Figure 3 compares plasma edge power density results versus major radius as derived from three different diagnostics. A tangential power density flow of 54 kW/cm^2, at a major radius of 193 cm, was inferred from the IR camera measurements of the limiter front face, which was at a 3.4^0 angle to the horizontal tangent of the plasma sheath. The results at major radii beyond the scoop front face were derived from calorimeter probe measurements located toroidally 90 ^{0} from the scoop limiter. Shown also are power density results, from TVTS electron temperature profiles measured at a major radius of 191 cm, at location 144 ^{0} toroidally from the scoop limiter. The point at 191 cm was the outermost TVTS measurement. The point at 193 cm is a straight-line extrapolation of the TVTS data. These plasma edge results derived from three different measurement techniques, at three different toroidal locations and major radii, exhibit a consistent trend over five orders of magnitude, and imply an effective 1/e power scrape-off length of 1.5 cm at the limiter surface. These results also imply a relatively high edge temperature, a relatively high edge power density near the limiter surface , and a small power flow to major radii beyond the limiter channels.

3.2 Temperature Profiles.

In general,. operating conditions were found for both ohmic- and neutral-beam-heated plasmas that yielded either symmetric or asymmetric horizontal midplane temperature profiles across the limiter front face. During constant heating conditions, most plasmas yielded limiter temperature profiles, whose intensity increased uniformly with time, the rate depending on total heating power, and whose symmetry remained constant during the pulse. The few plasmas that yielded time-varying changes in the symmetry of the limiter temperature profile exhibited disruptive MHD activity.

Ohmic-heated plasmas were found to yield thermal depositions that were most intense on either the ion drift side or the electron drift side of the limiter front face, depending on the operating conditions. There was a tendency for ohmically heated plasmas with less stable discharge conditions (i.e., disruptive MHD activity) to yield thermal depositions that were most intense on the electron drift side of the limiter front face, whereas, more favorable operating conditions tended to yield depositions that were most intense on the ion drift side.

In general, for both co- and counter-injected beams, the observed temperature profiles were most intense on the ion drift side of the limiter front face and this asymmetry tended to increase with beam power.

Figure 4 (a) shows a scoop limiter horizontal front face midplane asymmetric temperature profile for a 300 kA D^+ discharge heated for 300 msec with 1.4 MW of counter-injected D^0. The thermal deposition was greatest on the ion drift side of the limiter front face. Figure 4 (b) shows a scoop limiter front face midplane temperature profile for a 370 kA D^+ discharge heated for 300 msec with a co-injected 2.5 MW D^0. The thermal deposition was more symmetric about the center vertical of the limiter front face. The arrow at the right indicates ion drift direction for co-injected D^0. Figure 4 (c) shows a scoop limiter front face midplane temperature profile for a 350 kA D^+ discharge heated for 300 msec with 5.2 MW of co-injected D^0. The thermal deposition exhibited a maximum at the center and a maximum of comparable intensity on the ion drift side of the limiter front face. In general, as discussed above, the observed temperatures increased monotonically during the neutral-beam-heating pulse from the temperature levels achieved during the ohmic-heating phase. Figures 4a, 4b, and 4c display temperature profiles at the time of temperature maximum that occurred at the end of the neutral-beam-heating pulse.

In order to study the observed limiter front face thermal load asymmetries as a function of plasma parameters, the profiles were quantified in terms of the simultaneously occurring front face midplane peak center temperature (CT), the peak temperature at the electron drift side of the limiter (SE), and the peak temperature at the ion-drift-side of the limiter (SI). The above quantities were used to define the average midplane temperature (T_{av}), where

$$T_{av} = \frac{SE + CT + SI}{3} \qquad (1)$$

and the thermal load asymmetry (L_s), where

$$L_s = \frac{SI - SE}{SI + SE} \qquad (2)$$

and the peak temperature ratio (P_r), where

$$P_r = \frac{CT}{\frac{(SE + SI)}{2}} . \qquad (3)$$

3.3 Average Midplane Temperatures.

Figure 5 shows the average midplane front face temperature, as defined in Eq. (1), versus power absorbed by the plasma for 300 msec neutral beam pulses. The scatter is due in part to varied plasma conditions. In general, the average temperature appeared to increase with absorbed heating power. However, the thermal loads that were observed at the highest power levels near 5 MW also occurred under certain conditions at power levels of only 2 MW. There is not sufficient data to determine if this behavior represents a saturation in the power being transported to the scoop face. Normalization of the absorbed power to the line average density did not significantly change the behavior shown in Fig.5.

Figure 6 shows that, in general, plasmas depositing the highest thermal loads on the limiter had the shortest energy confinement times, in agreement with the observed degradation of confinement time with heating power absorbed by the plasma, as is also observed with conventional rail limiters. In addition, although as noted above, the ratio of power deposited on the limiter to total power absorbed by the plasma varied from 0.25 to 0.50 over the range of explored plasma conditions, this ratio was relatively constant for large variations in power absorbed and energy confinement times, during otherwise similar plasma conditions, as is also observed with rail limiters. Hence, in these aspects, the behavior of power transport to the scoop limiter was similar to that measured with conventional rail limiters.

Figure 7 shows the average midplane front face temperature versus the average Langmuir probe signals in the scoop limiter channels. These results indicate that as the particle flow into the limiter channels increased, the thermal transport to the limiter front face also increased.

3.4 Thermal Load Asymmetry.

As mentioned above, the symmetry of the thermal transport to the scoop limiter front face underwent interesting changes with various plasma conditions. Figure 8 shows the temperature or thermal transport symmetry, as defined in Eq. (2), versus absorbed power normalized to the line average density. It is seen that the asymmetry tended to increase on the ion drift side of the limiter front face with increasing absorbed power per particle.

Figure 9 shows the thermal load asymmetry versus energy confinement time. It is seen that longer confinement times were associated with more symmetric profiles. This appears to occur because the thermal load asymmetry tended to decrease with absorbed beam power, and there is a general improvement in confinement with decreasing beam power. Normalization of the energy confinement time to plasma current did not significantly change the behavior shown in Fig. 9 and indicates that the observed aysmmetries did not exhibit a strong dependence on plasma current.

The thermal load asymmetry was studied briefly versus the plasma vertical position. It is found that the asymmetry increased toward the ion drift direction as the plasma position was raised. There is not sufficient data to determine the asymmetry trend for lower plasma positions.

Figure 10 shows the thermal load symmetry versus the Langmuir probe signal symmetry in the scoop limiter channels. It is seen that while there is considerable scatter in the results, there may be a tendency towards increased plasma in the scoop channel facing the ion drift direction, as the asymmetry of the thermal load at the limiter front face increases toward the ion drift direction (positive L_s).

Figure 11 shows the average midplane front face temperature versus temperature profile symmetry. Symmetric profiles tend to be associated with lower front face temperatures. This is consistent with the trend toward more symmetric profiles and lower front face temperatures as the absorbed power decreases.

Relatively center-peaked temperature profiles were observed under some plasma conditions. This effect is suggestive of increased perpendicular transport or decreased scrape-off length and was studied using the peak ratio parameter (P_r) as defined in Eq. (3). This analysis showed little dependence on absorbed power and a large scatter in the results. The origin of this scatter and the interesting variations that occurred from shot to shot under apparently stable plasma conditions is not known at this time.

4.0 DISCUSSION AND SUMMARY.

The power transport to the scoop limiter front face, measured with the IR camera, was 25-50 % of the total heating power absorbed by the plasma (OH+ NB). The radiated and charge exchange power, measured with a 19-channel bolometer array along chords through the plasma was usually << 20-40 % of the total absorbed power. Estimates from calorimeter and Langmuir probes measurements imply that the power input to the scoop limiter channels was only about 3% of the total absorbed heating power. The result of assuming a toroidally and poloidally symmetric radiated power distribution yields a deficit in the power accountability of about 5-40% of the total power absorbed by the plasma. The origin of this deficit , which is on the order of those found for rail limiter discharges in PDX, has not been determined at this time but may have been due to asymmetries in the distribution of power radiated. Recent experiments on TFTR, for example, have shown evidence of toroidal asymmetries in the distribution of radiated power of up 20% due to the presence of the moveable outer limiter and poloidal asymmetries of up to 50% due to edge phenomena under some plasma conditions.[9]

A visual inspection of the scoop limiter after it was removed from the vessel indicated that the front face received minimal surface damage. The entire front face exhibited typical vertically rising arc tracks inclined about 5-10^0 toward the centerline, on each side of the centerline. The ion drift side for co-injection exhibited visual discoloration, but no obvious macroscopic erosion effects, or structural damage. This is indicative of intense, but not excessive, heating absorbed from the ion drift direction, and consistent with the range of observed front face temperatures and the majority of asymmetric temperature profiles. This evidence of minimal surface erosion is also consistent with bremsstrahlung and spectroscopic measurements. Central cord bremsstrahlung emission measurements yielded line averaged Z_{eff} of ≈ 1.5-2.3. Vacuum UV spectroscopic measurements found mainly low Z impurity lines which were predominantly carbon and oxygen at intensities comparable to divertor discharges. The role of scoop limiter surface interactions and the previously discussed [7] plasma near-edge relaxation phenomena consisting of 50-150 kHz quasicoherent density oscillations has not been determined.

Asymmetric temperature profiles and the filling-in of the valley between the temperature peaks have been observed previously on the DIII rail limiter,[10] the PDX inner toroidal limiter,[11] and the TFTR rail limiter.[12] The observed temperature profile asymmetries are strongly dependent on the respective particle density and temperature profiles in the scrape-off zone. The simple Schmidt model [13] for scrapeoff of power flow along field lines at a limiter predicts a symmetric double peaked temperature profile and a decreasing peak separation with a shortening of the scrape-off length. Using this model and the limiter surface geometry, the measured separation between the peak temperature points for typical double-peaked temperature profiles implies a 1/e energy scrape-off length of 1.5-cm. This is consistent with the power scrape-off length of 1.5-cm implied from TVTS, IR camera heat flux, and calorimeter probe results discussed above and shown in Fig. 3. The filling-in of the valley between peaks indicates the presence of radial transport, which is not included in the Schmidt model in an explicit manner. Fast ion orbits, finite Larmor radius effects, perpendicular diffusion, and sheath flow effects are candidate mechanisms for this perpendicular power transport. Analysis of a double-peaked 5 MW case using the inferred 1.5-cm energy scrape-off length implies 1.5 MW or 28% of the incident power is attributable to perpendicular transport. In the case of the strongly center-peaked profiles (e.g., Fig. 4B), it is difficult to resolve unambiguously the effects of radial transport and a possibly shortened scrape-off length. Strong variations in scrape-off length with edge conditions were observed previously[10-12] and are under extensive investigation.

The effect of beam particles lost to orbits extending outside of the limiter radius was investigated. Transport calculations were performed using a modified version of the TRANSP code [14] employing the actual vessel geometry, realistic neutral densities at the plasma edge, and a simple limiter geometry. The results yielded a limiter power deposition incident from the ion drift direction due to beam orbits extending outside of the limiter radius, corresponding to ≈ 20-40% of the total scoop limiter front face thermal load. Although this result is consistent with the magnitude and direction of the observed temperature profile asymmetries, this agreement may be fortuitious in view of the simplifying approximations that were employed.

Generally, the observed temperature profiles were relatively constant in shape from shot to shot, for relatively constant plasma conditions, but at times appeared to be sensitive to subtle changes in operating conditions. Although this interesting behavior is not sufficiently documented for additional quantitative studies, it suggests that real-time thermal load measurements may be helpful for optimizing plasma operation on scoop limiters.

ACKNOWLEDGMENTS

This work was supported by US Department of Energy Contract No. DE-AC02-76-CHO-3073. The authors wish to thank M. Egan, H. Richter, and the PDX technical crew and research staff for assistance and support in these experiments.

REFERENCES

1. P. Mioduszewski, "Experimental Studies on Pump Limiters," J. Nucl. Mater. **111 & 112**, 253 (1982), and references therein.
2. R.W. Conn, "Tokamak Pump Limiters," J. Nucl. Mater. **128 & 129**, 407 (1984), and references therein.
3. R. Budny *et al.*, "Designs for a Pumped Limiter System for TFTR," Princeton Plasma Physics Laboratory Report No. PPPL-2365 (1986).
4. R. Budny *et al.*, "Initial Results from the Scoop Limiter Experiment in PDX," J. Nucl. Mater. **121**, **294** (1984).
5. R. Budny *et al.*, "High Energy and Particle Confinement Times on PDX Scoop Discharges," J. Nucl. Mater. **128 & 129**, 425 (1984).
6. R.J. Fonck *et al.*, " Particle Fueling and Impurity Control in PDX," J. Nucl. Mater. **128 &129**, 330 (1984).
7. K. McGuire *et al.*, "Divertor and Scoop Limiter Experiments on PDX," in Proc. of Tenth Int. Conf. on Plasma Physics and Controlled Nuclear Fusion Research, London, UK, Sept. 1984.
8. R.Kaita *et al.*, " Charge Exchange Measurements of Beam Ion Thermalization in MHD-Quiescent Plasma in the Poloidal Divertor Experiment," Nucl. Fusion, 25, 939 (1985).
9. J. Schivell and C. E. Busch, " Radiative Power Loss in TFTR with Neutral Beam Heating and the Approach to the High Density Limit," Bull. Am. Phys. Soc. **30**, 1521(1985); C. E. Busch *et al.*, "Radiated Power from Ohmically Heated TFTR Plasmas," Bull. Am Phys. Soc. **30**, 1517 (1985); J.Schivell *et al.*, "Analysis of Highly Asymmetric Radiation Loss Profiles in TFTR," Proc. of the 6th on

Topical Conf. on High Temp. Plasma Diagnostics, Hilton Head, SC, March 1986 (to be published in Rev. Sci. Instr.).

10. T. Taylor, N. Brooks, and K. Ioki, " Changes in Limiter Surface Temperature Profiles for Small Radius Plasmas in Doublet III," J. Nucl. Mater., **111 &112**, 569 (1982).

11. M. Ulrickson and H.W. Kugel, " Initial Temperature Profiles on the PDX Inner Toroidal Limiter," Nucl.Technol./Fusion, 4,141 (1983).

12. M. Ulrickson, C. Bush, S. Medley, and J. Schivell, " Power Balance in TFTR," Bull. Am. Phys. Soc. **30**, 1520 (1986).

13. J. A. Schmidt, "Tokamak Impurity Control Techniques," in "Comments on Plasma Physics and Controlled Fusion" 5, 225 (1980).

14. R.T. McCann *et al.*, " Inclusion of FLR Effects in the TRANSP Beam Model," Bull. Am. Phys. Soc. 28, 1222 (1983).

FIGURE CAPTIONS

FIG.1 Schematic plan view of the PDX scoop limiter showing the channels, neutralizer, and diagnostics.

Fig.2 Schematic elevation view of the PDX scoop limiter blades and ion side entrance channel.

FIG.3 Plasma edge power density (kW/cm^2) versus major radius (cm) as inferred from IR camera measurements, calorimeter probe measurements, and TVTS profile measurements.

FIG.4(a) A front face, horizontal midplane, asymmetric temperature profile for a 300 kA D^+ discharge heated for 300 msec with 1.4 MW of counter-injected D^0. The thermal deposition is greatest on the ion drift side.

FIG.4(b) A front face, horizontal midplane, symmetric temperature profile for a 370 kA D^+ discharge heated for 300 msec with 2.5 MW of co-injected D^0. The arrow indicates the ion drift direction.

FIG.4(c) A front face, horizontal midplane temperature profile for a 350 kA D^+ discharge heated for 300 msec with 5.2 MW of co-injected D^0.

FIG.5 Average front face midplane temperature (T_{av}) versus absorbed power (P_{abs}) in MW.

FIG.6 The average front face midplane temperature (T_{av}) versus energy confinement time (T_e) in msec.

FIG.7 The average front face midplane temperature (T_{av}) versus the average of Langmuir probe signals (volts) in the scoop limiter channels.

FIG.8 The temperature profile or thermal load symmetry (L_s) versus absorbed power (P_{abs}) normalized to line average electron density (n_e).

FIG.9 Thermal load symmetry (L_s) versus energy confinement time (T_e) in msec.

FIG.10 Thermal load symmetry (L_s) versus the Langmuir probe signal symmetry between the limiter channels.

FIG.11 Average front face midplane temperature (T_{av}) versus temperature profile symmetry (L_s).

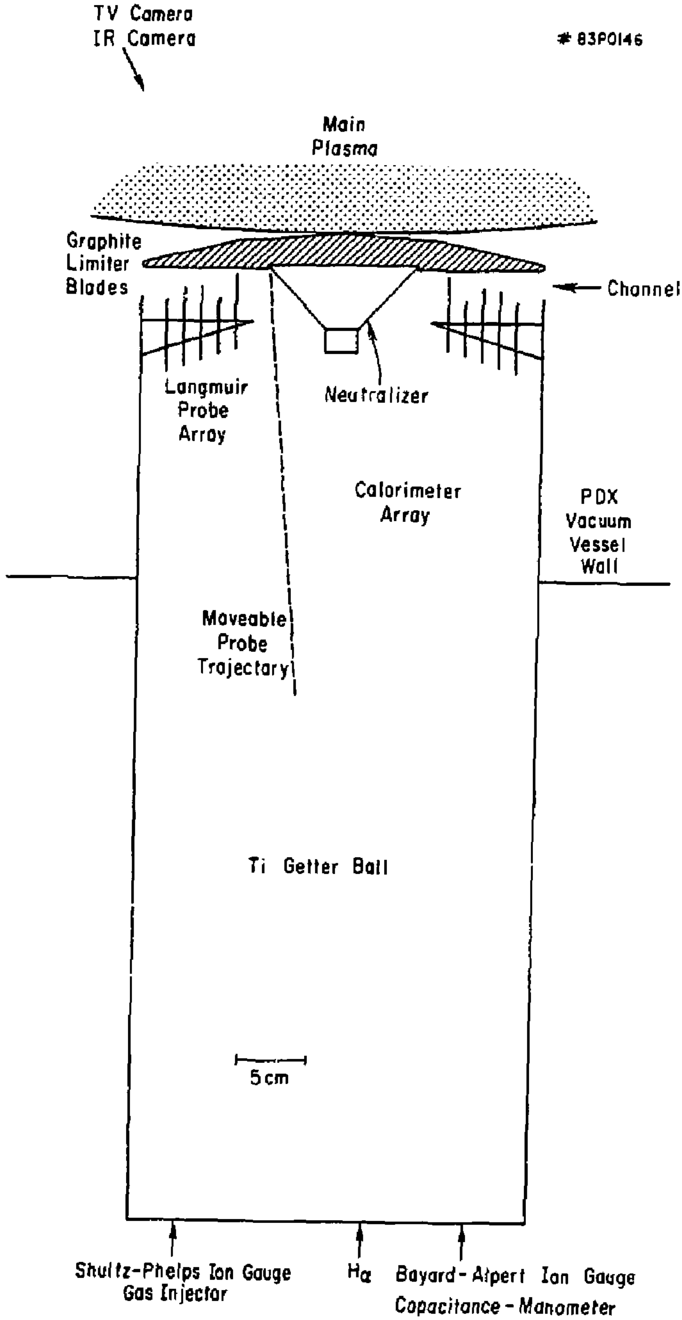
TV Camera
IR Camera
83P0146
Main
Plasma
Graphite
Limiter
Blades
Channel
Langmuir
Probe
Array
Neutralizer
Calorimeter
Array
PDX
Vacuum
Vessel
Wall
Moveable
Probe
Trajectory
Ti Getter Ball
5 cm
Shultz-Phelps Ion Gauge
Gas Injector
Hα
Bayard-Alpert Ion Gauge
Capacitance-Manometer

Fig. 1

#83P0137

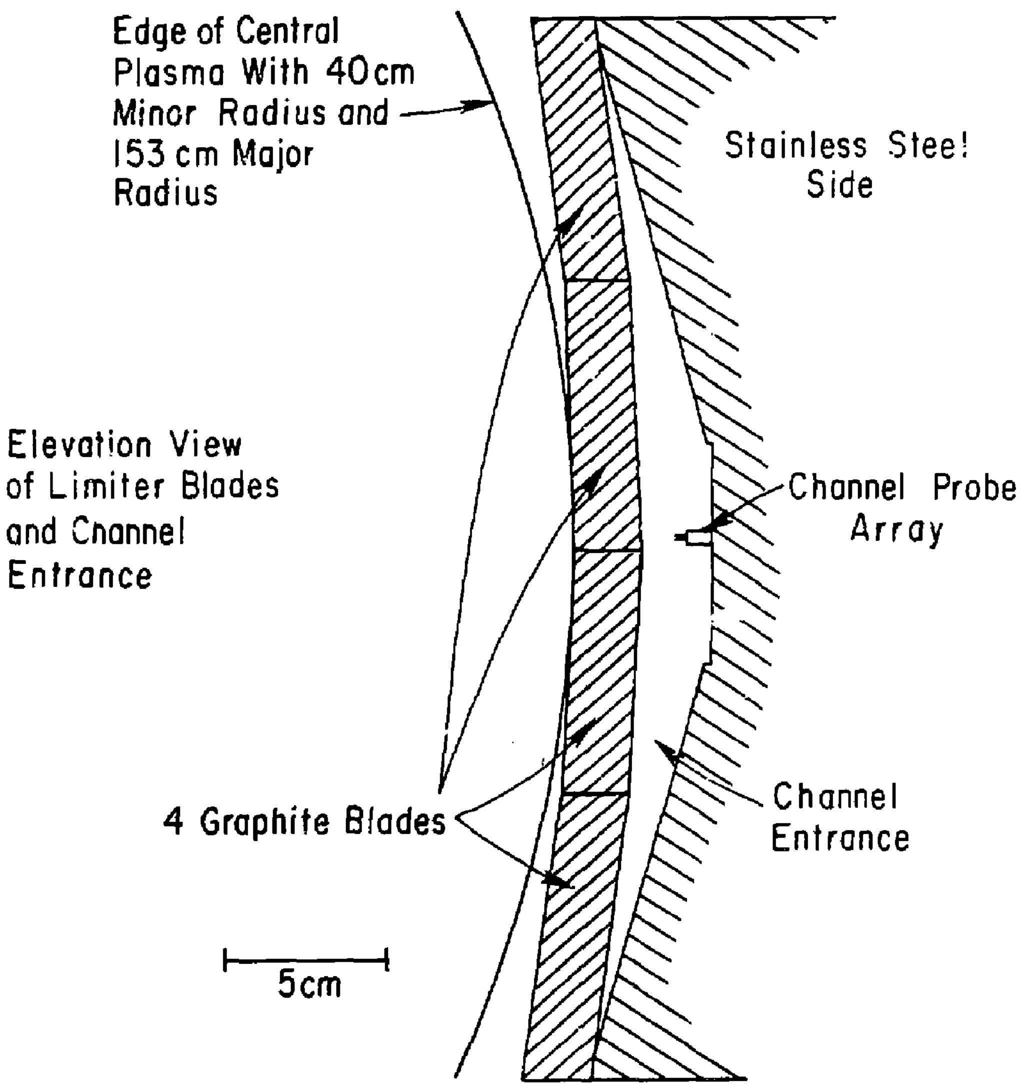

Fig. 2

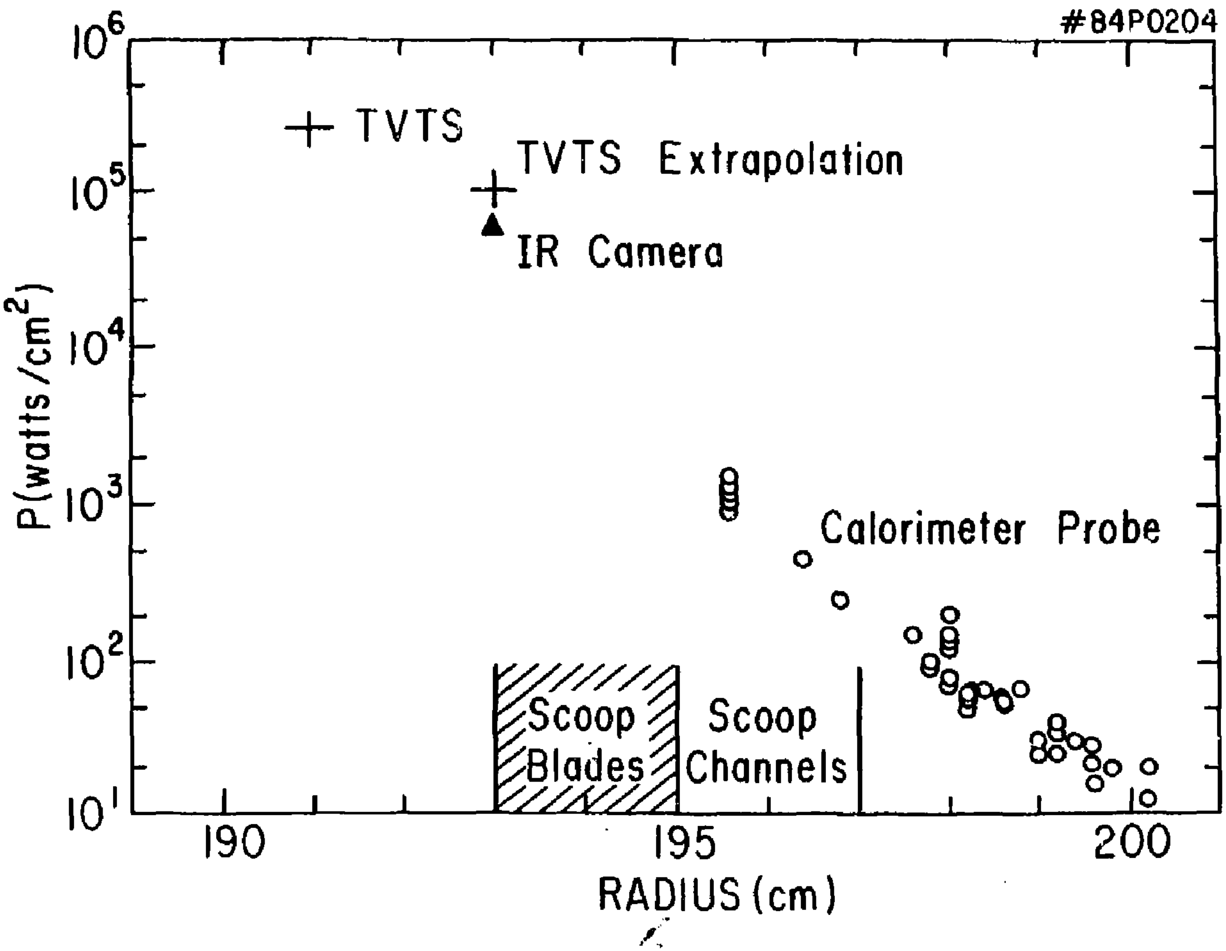
#84P0204
TVTS
TVTS Extrapolation
IR Camera
Calorimeter Probe
Scoop Blades
Scoop Channels
P(watts/cm²)
RADIUS (cm)
10⁶
10⁵
10⁴
10³
10²
10¹
190
195
200

Fig. 3

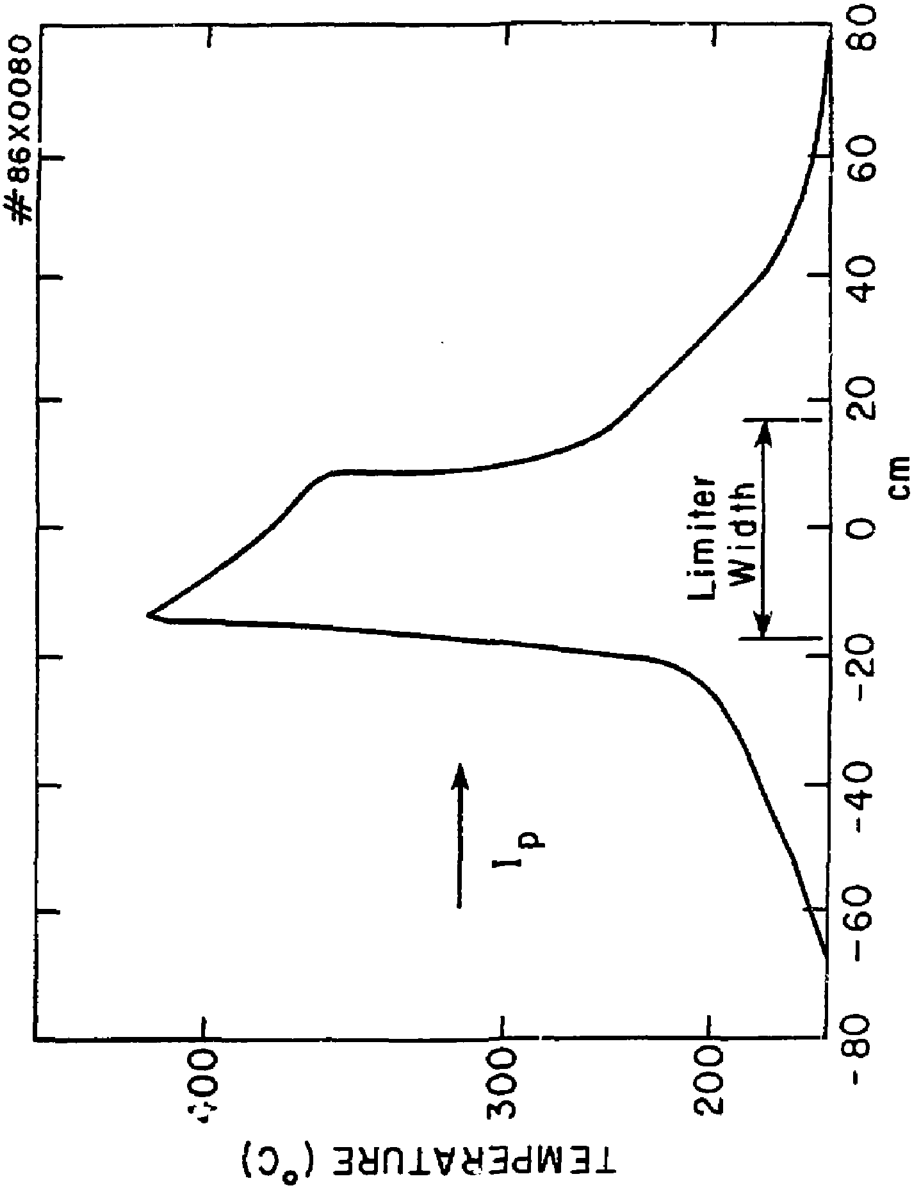
#86X0080
TEMPERATURE (°C)
400
300
200
-80
-60
-40
-20
0
20
40
60
80
cm
Limiter
Width
I_p

Fig. 4A

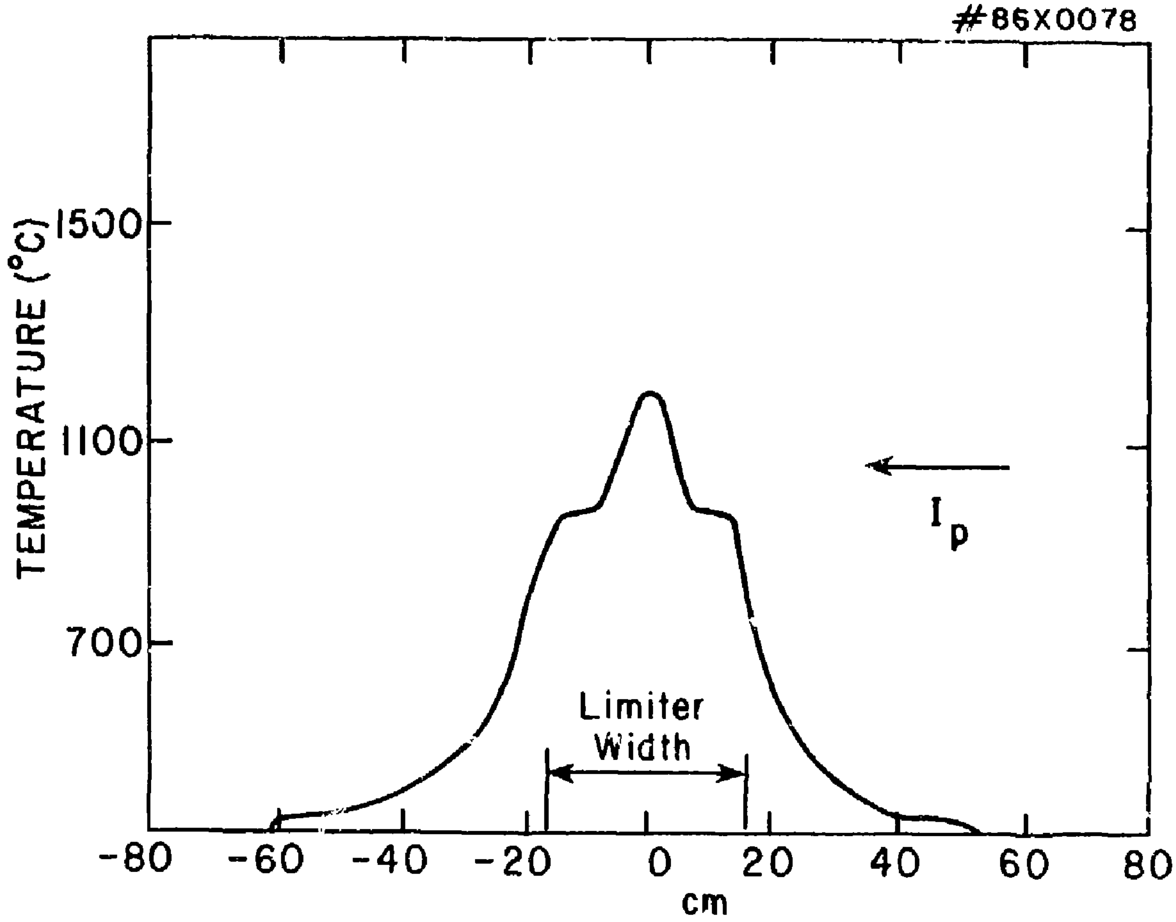
#86X0078
TEMPERATURE (°C)
1500
1100
700
Limiter
Width
I_p
-80
-60
-40
-20
0
20
40
60
80
cm

Fig. 4B

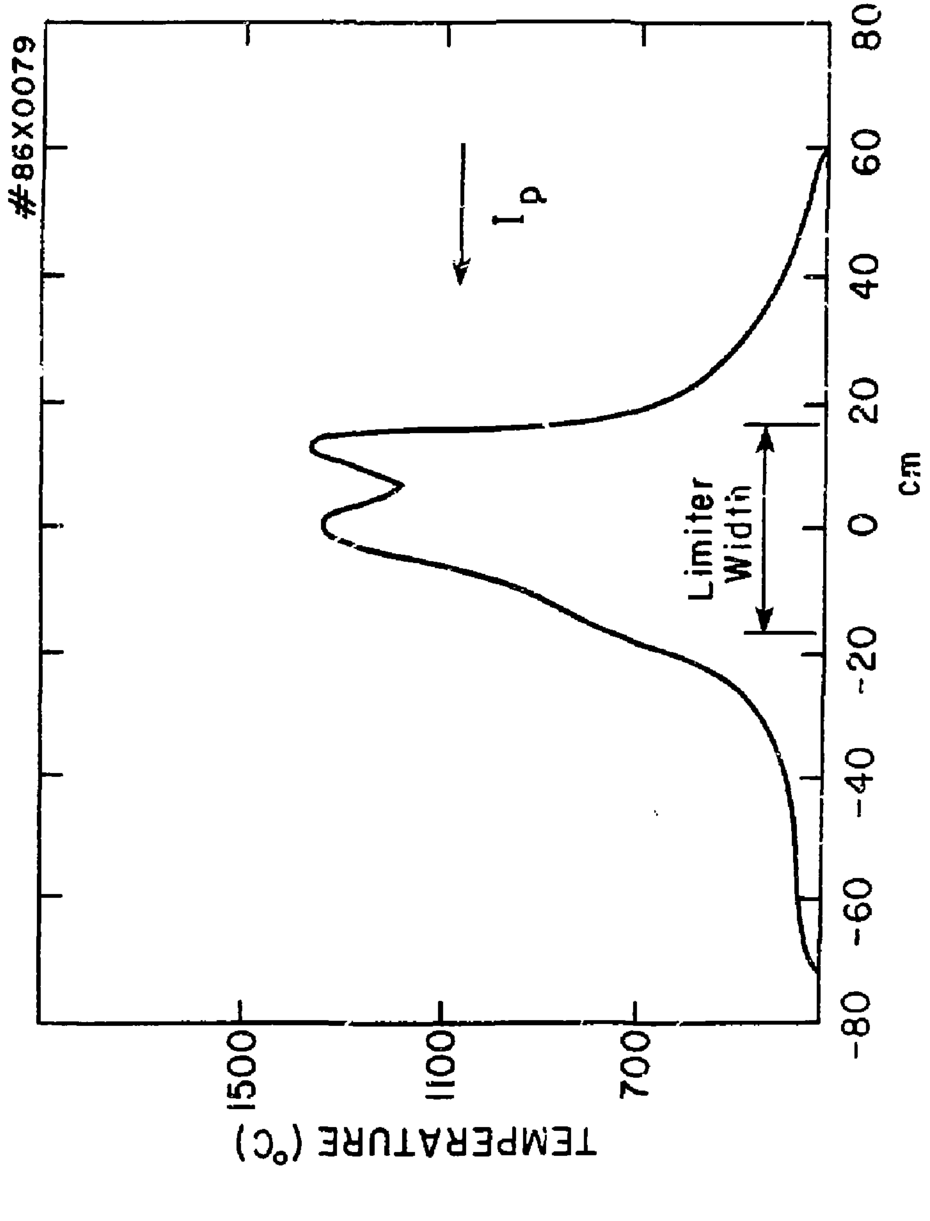
#86X0079
TEMPERATURE (°C)
1500
1100
700
-80
-60
-40
-20
0
20
40
60
80
cm
I_p
Limiter
Width

Fig. 4C

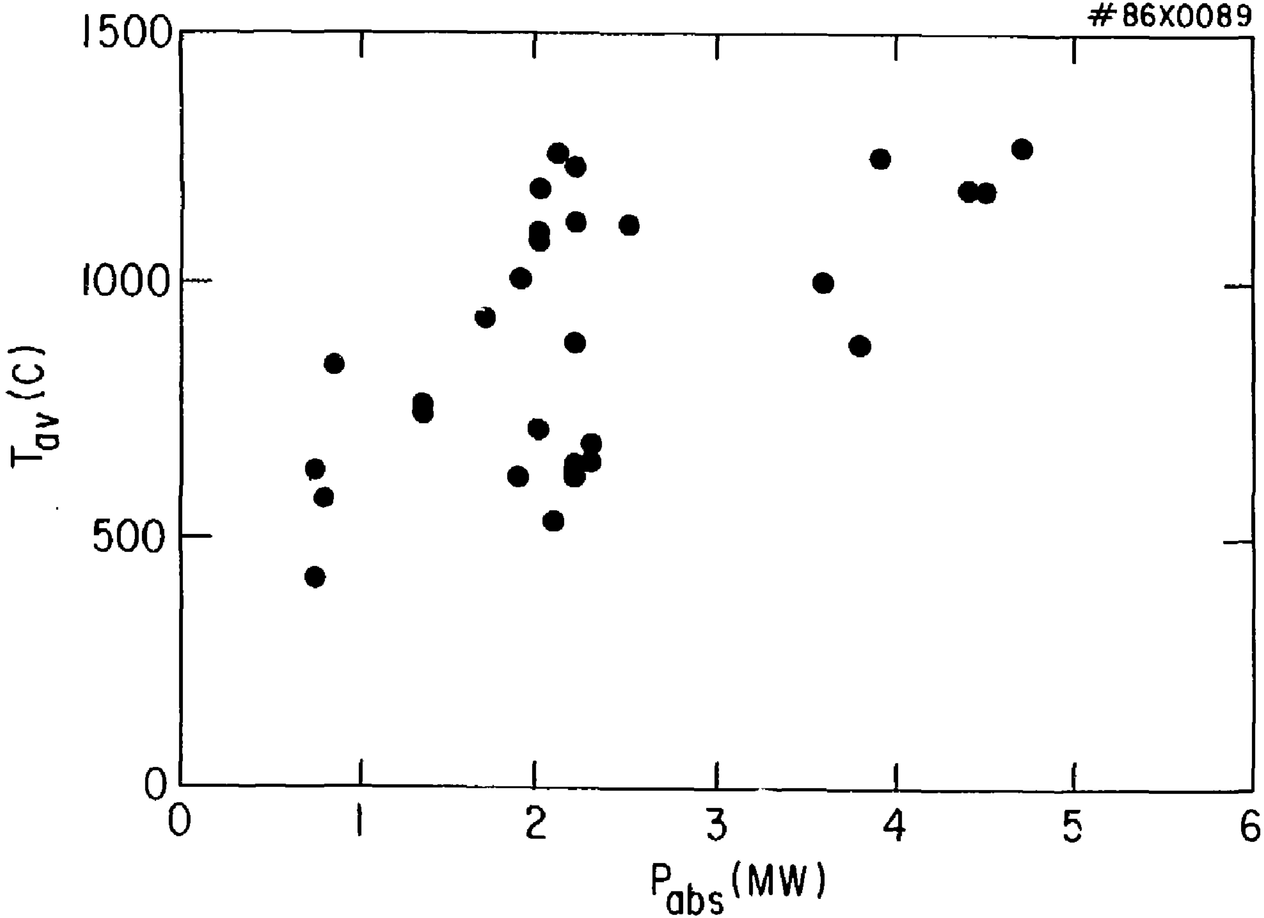

Fig. 5

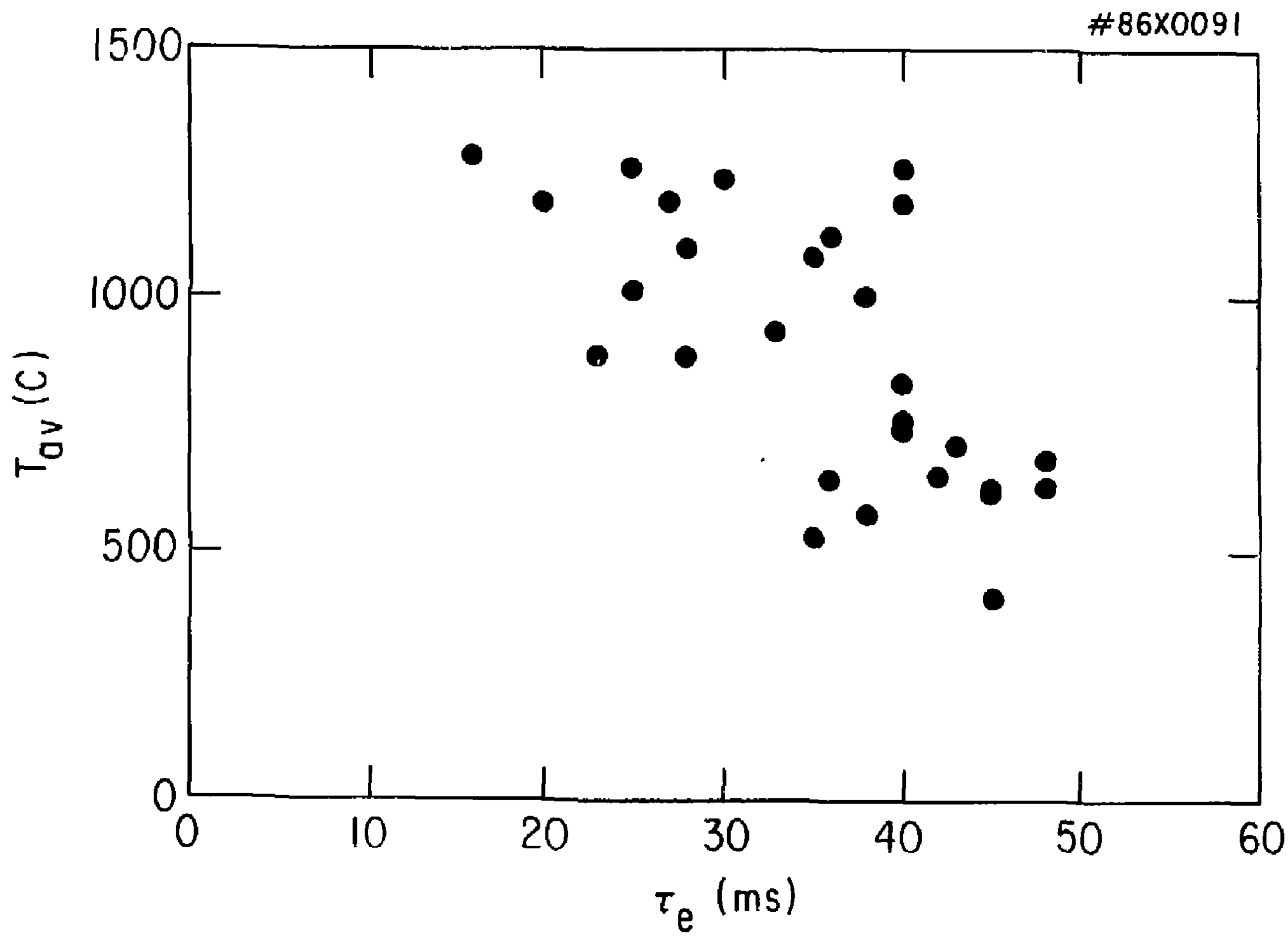

Fig. 6

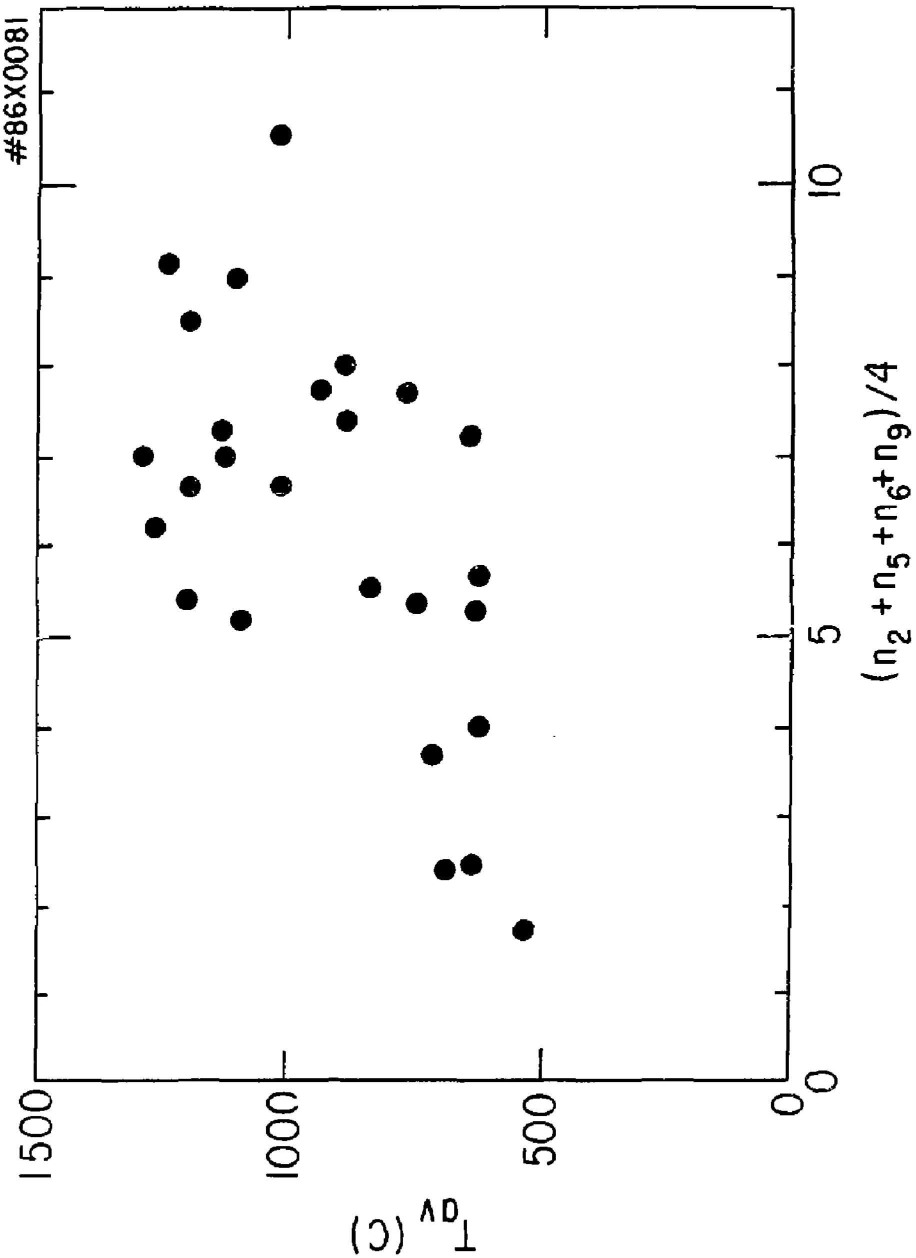

Fig. 7

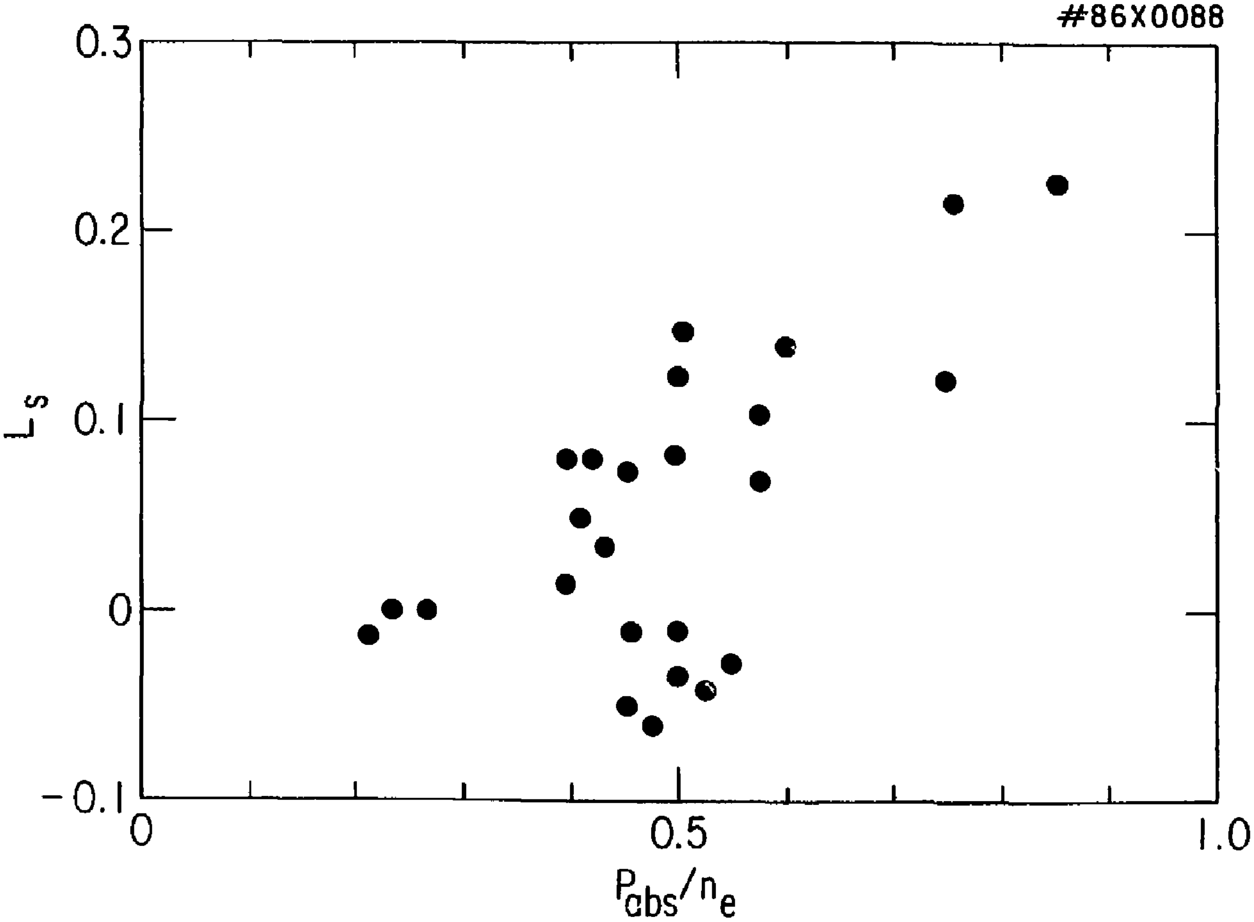

Fig. 8

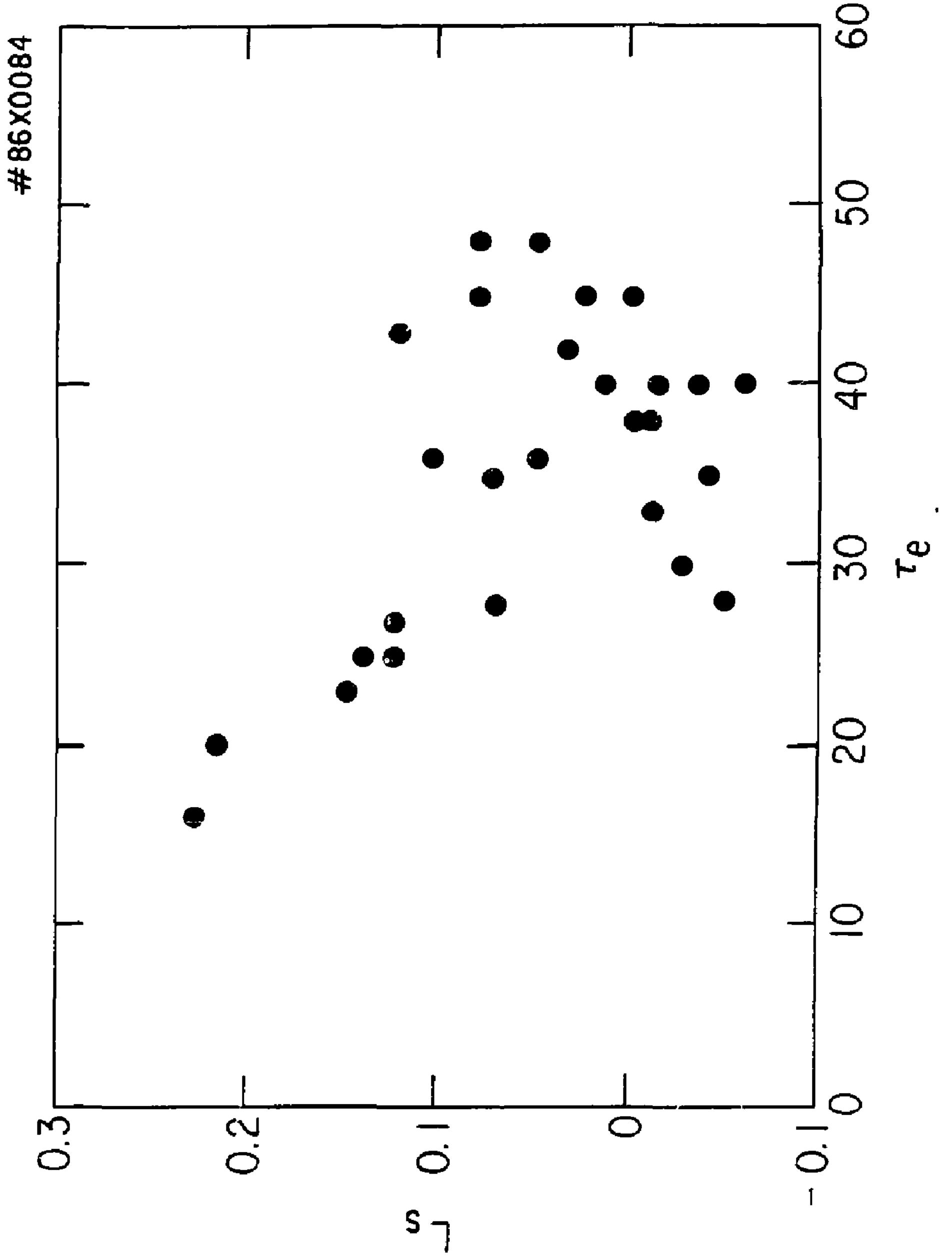

Fig. 9

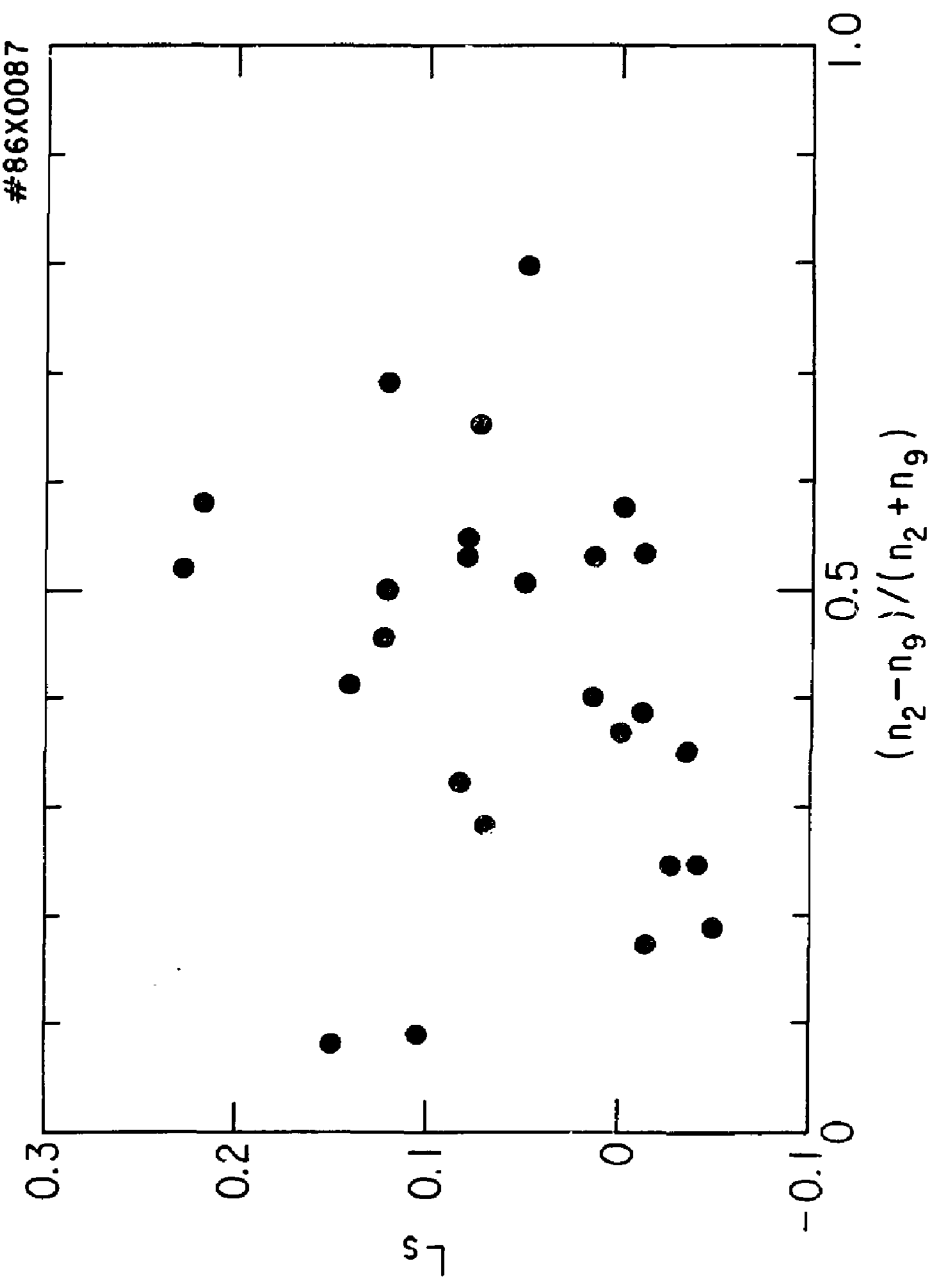

Fig. 10

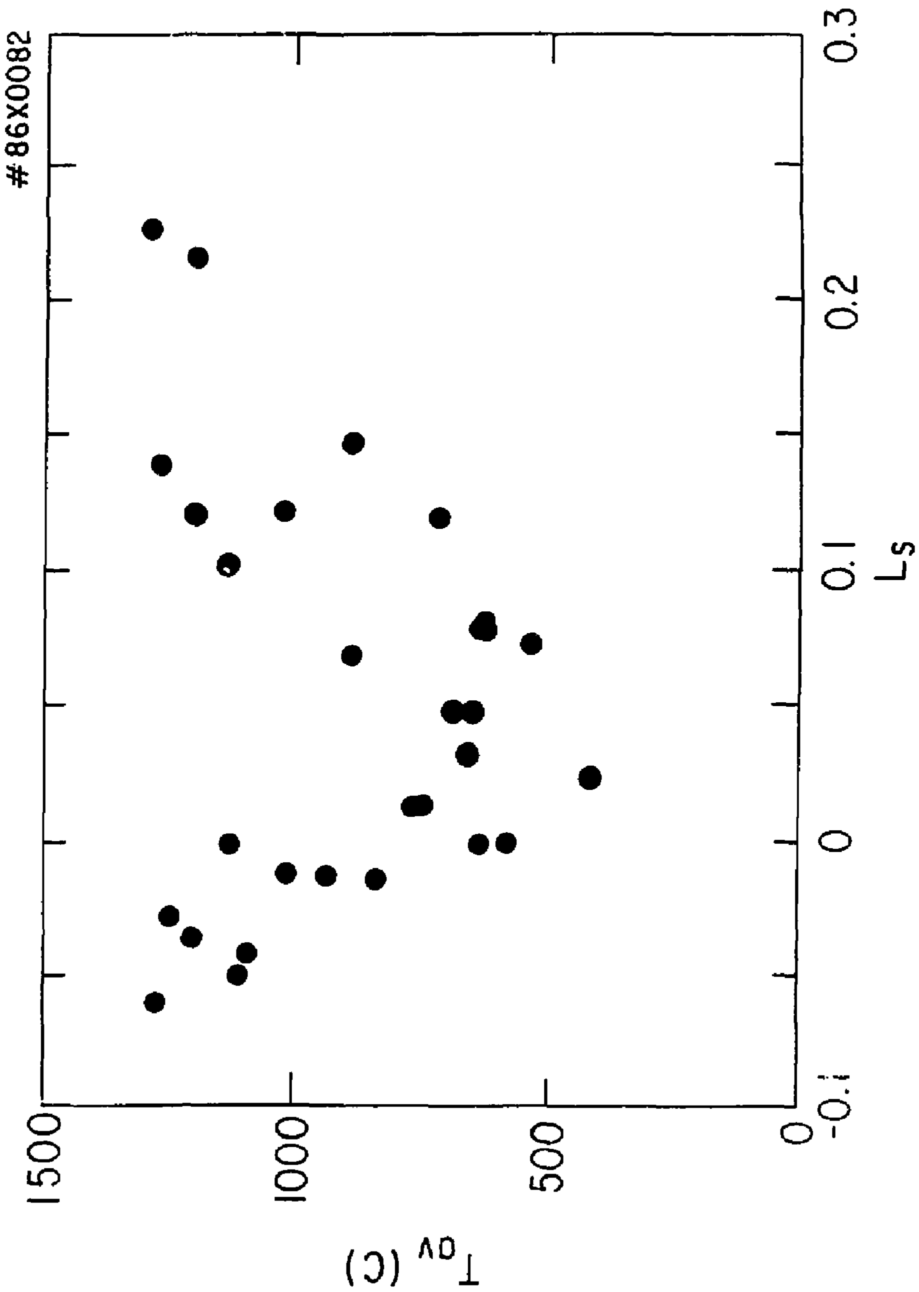

Fig. 11

EXTERNAL DISTRIBUTION IN ADDITION TO UC-20

Plasma Res Lab, Austra Nat'l Univ, AUSTRALIA
Dr. Frank J. Paoloni, Univ of Wollongong, AUSTRALIA
Prof. I.R. Jones, Flinders Univ., AUSTRALIA
Prof. M.H. Brennan, Univ Sydney, AUSTRALIA
Prof. F. Cap, Inst Theo Phys, AUSTRIA
M. Goossens, Astronomisch Instituut, BELGIUM
Prof. R. Boucique, Laboratorium voor Natuurkunde, BELGIUM
Dr. D. Palumbo, Dg XII Fusion Prog, BELGIUM
Ecole Royale Militaire, Lab de Phys Plasmas, BELGIUM
Dr. P.H. Sakanaka, Univ Estadual, BRAZIL
Lib. & Doc. Div., Instituto de Pesquisas Espaciala, BRAZIL
Dr. C.R. James, Univ of Alberta, CANADA
Prof. J. Teichmann, Univ of Montreal, CANADA
Dr. H.M. Skarsgard, Univ of Saskatchewan, CANADA
Prof. S.R. Sreenivasan, University of Calgary, CANADA
Prof. Tudor W. Johnston, INRS-Energie, CANADA
Dr. Hannes Barnard, Univ British Columbia, CANADA
Dr. M.P. Bachynski, MPB Technologies, Inc., CANADA
Chalk River, Nucl Lab, CANADA
Zhengwu Li, SW Inst Physics, CHINA
Library, Tsing Hua University, CHINA
Librarian, Institute of Physics, CHINA
Inst Plasma Phys, Academia Sinica, CHINA
Dr. Peter Lukac, Komenskeho Univ, CZECHOSLOVAKIA
The Librarian, Culham Laboratory, ENGLAND
Prof. Schatzman, Observatoire de Nice, FRANCE
J. Radet, CEN-BP6, FRANCE
JET Reading Room, JET Joint Undertaking, ENGLAND
AM Dupas Library, AM Dupas Library, FRANCE
Dr. Tom Mual, Academy Bibliographic, HONG KONG
Preprint Library, Cent Res Inst Phys, HUNGARY
Dr. R.K. Chhajlani, Vikram Univ. INDIA
Dr. B. Dasgupta, Saha Inst, INDIA
Dr. P. Kaw, Physical Research Lab, INDIA
Dr. Phillip Rosenau, Israel Inst Tech, ISRAEL
Prof. S. Cuperman, Tel Aviv University, ISRAEL
Prof. G. Rostagni, Univ Di Padova, ITALY
Librarian, Int'l Ctr Theo Phys, ITALY
Miss Clelia De Palo, Assoc EURATOM-ENEA, ITALY
Biblioteca, del CNR EURATOM, ITALY
Dr. H. Yamato, Toshiba Res & Dev, JAPAN
Direc. Dept. Lg. Tokamak Dev. JAERI, JAPAN
Prof. Nobuyuki Inoue, University of Tokyo, JAPAN
Research Info Center, Nagoya University, JAPAN
Prof. Kyoji Nishikawa, Univ of Hiroshima, JAPAN
Prof. Sigeru Mori, JAERI, JAPAN
Prof. S. Tanaka, Kyoto University, JAPAN
Library, Kyoto University, JAPAN
Prof. Ichiro Kawakami, Nihon Univ, JAPAN
Prof. Satoshi Itoh, Kyushu University, JAPAN
Dr. D.I. Choi, Adv. Inst Sci & Tech, KOREA
Tech Info Division, KAERI, KOREA
Bibliotheek, Fom-Inst Voor Plasma, NETHERLANDS
Prof. B.S. Liley, University of Waikato, NEW ZEALAND
Prof. J.A.C. Cabral, Inst Superior Tecn, PORTUGAL
Dr. Octavian Petrus, ALI CUZA University, ROMANIA
Prof. M.A. Hellberg, University of Natal, SO AFRICA
Dr. Johan de Villiers, Plasma Physics, Nucor, SO AFRICA
Fusion Div. Library, JEN, SPAIN
Prof. Hans Wilhelmson, Chalmers Univ Tech, SWEDEN
Dr. Lennart Stenflo, University of UMEA, SWEDEN
Library, Royal Inst Tech, SWEDEN
Centre de Recherchesen, Ecole Polytech Fed, SWITZERLAND
Dr. V.T. Tolok, Kharkov Phys Tech Ins, USSR
Dr. D.D. Ryutov, Siberian Acad Sci, USSR
Dr. G.A. Eliseev, Kurchatov Institute, USSR
Dr. V.A. Glukhikh, Inst Electro-Physical, USSR
Institute Gen. Physics, USSR
Prof. T.J.M. Boyd, Univ College N Wales, WALES
Dr. K. Schindler, Ruhr Universität, W. GERMANY
ASDEX Reading Rm, IPP/Max-Planck-Institut fur Plasmaphysik, F.R.G.
Nuclear Res Estab, Julich Ltd, W. GERMANY
Librarian, Max-Planck Institut, W. GERMANY
Bibliothek, Inst Plasmaforschung, W. GERMANY
Prof. R.K. Janev, Inst Phys, YUGOSLAVIA